Mobility enhancement of CVD graphene by spatially correlated charges

2017 2D Mater. 4 025026

(http://iopscience.iop.org/2053-1583/4/2/025026)

2D Materials

OPEN ACCESS

RECEIVED
12 October 2016

REVISED
13 December 2016

ACCEPTED FOR PUBLICATION
23 December 2016

PUBLISHED
1 February 2017

PAPER

Mobility enhancement of CVD graphene by spatially correlated charges

Lyudmila Turyanska[1,2], Oleg Makarovsky[1], Laurence Eaves[1], Amalia Patanè[1] and Nobuya Mori[3]

[1] School of Physics and Astronomy, The University of Nottingham, Nottingham, NG7 2RD, UK
[2] School of Chemistry, University of Lincoln, Lincoln, LN6 7DL, UK
[3] Division of Electrical, Electronic and Information Engineering, Graduate School of Engineering, Osaka University, Osaka, Japan

E-mail: Lyudmila.Turyanska@nottingham.ac.uk

Keywords: grapheme, spatial correlation of charges, mobility, quantum dots, PbS

Supplementary material for this article is available online

Abstract

We present a strategy for enhancing the carrier mobility of single layer CVD graphene (CVD SLG) based on spatially correlated charges. Our Monte Carlo simulations, numerical modeling and the experimental results confirm that spatial correlation between defects with opposite charges can provide a means to control independently the carrier concentration and mobility of planar field effect transistors in which graphene is decorated with a layer of colloidal quantum dots (QDs). We show that the spatial correlation between electrically charged scattering centres close to the graphene/SiO_2 interface and the localised charges in a QD layer can smooth out the electrostatic potential landscape, thus reducing scattering and enhancing the carrier mobility. The QD capping molecules influence the distribution and correlation of electrical charges in the vicinity of SLG and provide a means of tuning the carrier concentration and increasing the carrier mobility in graphene. These results represent a significant conceptual advance and provide a novel strategy for control of the electronic properties of 2D materials that could accelerate their utilization in optoelectronic devices.

Advances in the physics and technology of graphene (single layer graphene, SLG) have led to a wide range of fundamental discoveries and applications, which exploit its unique electrical properties, strength, transparency and mechanical flexibility, leading to device applications ranging from Thz devices [1] and ultrasensitive photon detectors [2, 3] to touch screens and wearable technology [4]. To date, the high room temperature carrier mobility of the exfoliated graphene (>10 $m^2 (Vs)^{-1}$) [5, 6] cannot be reproduced in SLG grown by scalable large area methods, e.g. low pressure chemical vapour deposition (LP-CVD) [7, 8] or thermal annealing of SiC [9]. The reduced mobility in CVD-grown SLG is usually attributed to the presence of crystalline defects and scattering of free carriers by charged impurities and mechanical deformations in the graphene layer [10]. Understanding the processes that control and limit the electrical properties of graphene is a challenging research field that has potential to accelerate the technological readiness of large area SLG. Recent work has demonstrated significant changes in the charge concentration and mobility of SLG following plasma-based treatment [7] and surface functionalisation with organic molecules [11, 12], ionic liquids [13, 14] and nanomaterials [2, 3, 15, 16]. Despite extensive work on the enhanced properties of decorated SLG devices, the mechanisms that govern the effect of surface functionalization on carrier density and mobility in SLG are not yet fully understood and controlled.

In this paper we demonstrate theoretically and experimentally that the correlation of charges in surface-functionalised graphene can provide a means to independently control the carrier concentration and mobility. Our electrostatic model and Monte-Carlo simulations indicate that surface decoration of graphene with localised charges can lead to either a reduction or an increase of the SLG carrier mobility, depending on the degree of charge correlation. In particular, the spatial correlation between electrically charged scattering centres located at the graphene/substrate interface and the localised charges in a capping layer can smooth out the electrostatic potential landscape, thus reducing scattering of charge carriers and enhancing their mobility. In order to achieve experimentally the spatial correlation-induced enhancement of mobility, we use CVD SLG devices decorated with a layer of

colloidal PbS quantum dots (QDs), which are passivated with different capping molecules. We show that the QD capping molecules influence the distribution and correlation of electrical charges in the vicinity of SLG and provide a means of tuning the carrier concentration and increasing the carrier mobility in graphene.

For SLG devices in which CVD-grown graphene is transferred onto a SiO_2/Si (300 nm) substrate, the presence of charged defects in the vicinity of the graphene layer has a major impact on the electrical properties [17]. Our devices are produced from CVD grown graphene; its single layer nature is confirmed by Raman spectroscopy [18]. The devices have linear current–voltage characteristics, with *p*-type conductivity at zero gate voltage, a measured carrier concentration, $p_0 = 1.7 \times 10^{16}$ m^{-2}, and field effect mobility, $\mu_0 = 0.5$ m^2 (Vs)$^{-1}$ at $T = 300$ K [19]. Here we show theoretically and experimentally that this mobility can be significantly increased by decorating the SLG with a layer of QDs.

We use a simple model to describe the effect of a QD layer deposited on the surface of CVD-SLG. It includes the spatial correlation between the negative ionized acceptor impurities at the SiO_2/SLG interface and the positively charged QDs, which behave as donors [19]. We define $\langle r_{\mathrm{imp}} \rangle$ as an average nearest neighbour distance between impurities, $\langle d_{\mathrm{min}} \rangle$ as an averaged minimum in-plane distance between the QDs and impurity charges, and r_{max} as a maximum allowed QD-impurity distance (figure 1(a), and supplementary information S1–S3 (stacks.iop.org/TDM/4/025026/mmedia)). Then the degree of spatial correlation can be described by the correlation coefficient $\beta = \langle d_{\mathrm{min}} \rangle / \langle r_{\mathrm{imp}} \rangle$. Here $\beta = 0$ corresponds to the maximum spatial correlation with $\langle d_{\mathrm{min}} \rangle = 0$, and $\beta = 1$ describes uncorrelated distribution of QDs and impurities with $\langle d_{\mathrm{min}} \rangle = \langle r_{\mathrm{imp}} \rangle$.

Figure 1(b) shows the electrostatic potential in the SLG calculated as a sum of Coulomb potentials generated by the impurities and the QDs for different values of β. The screening effect of graphene is neglected as the carrier concentration in the investigated samples is low. To calculate the potential maps shown in figure 1(b), we consider the case where the number of randomly distributed impurities and of QDs is equal to the carrier concentration measured in our pristine graphene, i.e. $N_{\mathrm{imp}} = N_{\mathrm{QD}} = p_0 = 1.7 \times 10^{16}$ m^{-2} and $\langle r_{\mathrm{imp}} \rangle = (4N_{\mathrm{imp}})^{-1/2} = 3.8$ nm. In our model the QDs are placed randomly within an area of radius r_{max} from each impurity (insert in figure 1(c)). Reducing r_{max} leads to a corresponding reduction of $\langle d_{\mathrm{imp}} \rangle$ and β. The dependence of the correlation parameter β on r_{max} is shown in figure 1(c) (for details see supplementary materials, S1–S3).

Electrostatic potential maps for the cases of strong ($\beta = 0.25, r_{\mathrm{max}} = 2$ nm), medium ($\beta = 0.60, r_{\mathrm{max}} = 6$ nm) and no correlation ($\beta = 1$, $r_{\mathrm{max}} = 100$ nm) are shown in figure 1(b). It can be seen that there is a strong decrease of the length and depth of electrostatic fluctuations for the highly correlated cases. These fluctuations are characterised by a standard deviation $\sigma = \sqrt{\frac{1}{N}\sum_{i=1..N}(U_i - \langle U \rangle)^2}$, where U_i and $\langle U \rangle$ are the local and mean values of the electrostatic potential energy, and N is the number of local points where this potential is defined. The values of σ are 186 meV, 85 meV and 45 meV for $r_{\mathrm{max}} = 100$ nm, 6 nm and 2 nm, respectively.

Monte Carlo simulations were performed to estimate the effect of the spatial correlation of charges on the carrier mobility, μ (see supplementary information, S4). Figure 2(a) compares the calculated dependence of the impurity-limited mobility, μ_{imp}, on N_{imp} according to a simple analytic expression for the mobility in extrinsic graphene proposed by Adam *et al* [22], i.e.

$$\frac{\mu_{\mathrm{imp}}}{\mu_0} = \alpha \frac{N_0}{N_{\mathrm{imp}}}, \qquad (1)$$

where $\mu_0 = 1$ m^2 (Vs)$^{-1}$, $N_0 = 10^{14}$ m^{-2} and α is a phenomenological parameter [22]. Our Monte Carlo simulations of μ_{imp} are in qualitative agreement with this model for $\alpha = 150$. In the case of an impurity-free SLG layer, the carrier mobility calculated by Monte Carlo simulations is limited by phonon scattering with maximum phonon-limited mobility of $\mu_{\mathrm{ph}} \approx 20$ m^2 (Vs)$^{-1}$ at room temperature (supplementary information, S5). The concentration of impurities and mobility in our pristine graphene ($\mu_{\mathrm{pristine}} = 0.5$ m^2 (Vs)$^{-1}$) corresponds to the red circle in figure 2(a). We now examine the effect of the correlation of charges on mobility. The calculated dependence of μ on the correlation length, r_{max}, is shown in figure 2(b) for a stand-off impurity-SLG distance $z_{\mathrm{imp}} = 1$ nm [22] and a QD-SLG separation $z_{\mathrm{QD}} = 1$ nm, 5 nm and 10 nm (see supplementary information, S1). Our Monte Carlo simulations clearly indicate that the mobility in SLG depends on the degree of spatial correlation between positive and negative charges. A similar mechanism has been proposed previously to explain the increase of carrier mobility in conventional bulk semiconductors [20, 21].

We note that for large correlation lengths, $r_{\mathrm{max}} > 20$ nm, the randomly distributed positive charges introduce an additional Coulomb scattering, leading to a decrease of mobility relative to that of pristine graphene (lower dashed line in figure 2(b)). In contrast, for stronger spatial correlations, $r_{\mathrm{max}} < 10$ nm, the carrier mobility is significantly higher. In particular, for $r_{\mathrm{max}} \sim 1$ nm, the electrostatic potentials maps reveal a strong reduction in the amplitude of the potential fluctuations (figure 1(b)), leading to a reduction of carrier scattering. Our calculations indicate that at $r_{\mathrm{max}} < 1$ nm and $z_{\mathrm{QD}} = 1$ the mobility approaches its phonon-limited maximum value of ≈ 20 m^2 (Vs)$^{-1}$ (figure 2(b)).

In order to explore the effect of the spatial correlation of charges in SLG experimentally, we fabricated the CVD graphene into 2-terminal devices and decorated them with a layer of colloidal PbS QDs with average nanocrystal diameter $d_{\mathrm{PbS}} \approx 4$ nm passivated by different capping ligands (figure 3(a), experimental

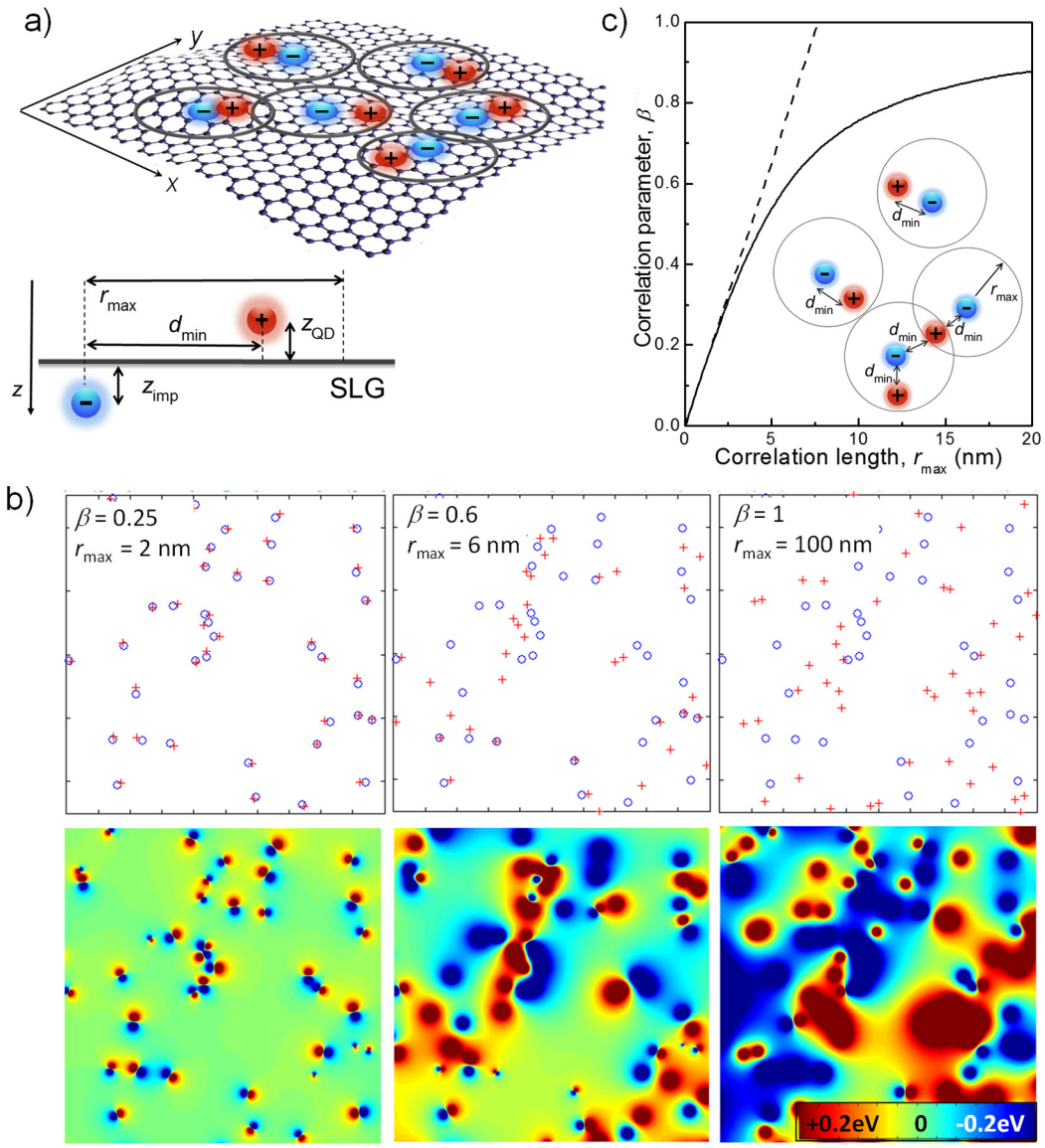

Figure 1. (a) Illustration of spatial correlation between local charges in the vicinity of the graphene plane in the *xy*-plane and (inset) vertical *z*-direction. (b) Simulated positions of impurity (blue o) and QD (red +) charges within the *xy*-plane of an area 50 μm × 50 μm for different correlation lengths, r_{max}, and corresponding electrostatic potential maps in graphene. (c) Correlation parameter β as a function of r_{max} and (inset) a sketch of distribution of charges in the *xy*-plane. The dashed line is for $\beta = r_{max}\sqrt{N_{imp}}$.

section). The length, l, of the capping ligand determines the spatial separation between individual nanocrystals and between them and the SLG. The overall QD size is estimated as $d_{QD} = d_{PbS} + 2l$. We note that our devices are decorated with as-synthesised QDs and the QD layer does not undergo any chemical modifications [23]. Our measurements indicate that the presence of the layer of capping molecules between the SLG and the nanocrystals allows charge transfer into the adjacent graphene film but does not enable a measurable electrical conductance parallel to the plane of the device. We estimate the areal surface density of QDs assuming hexagonal packing, where $N_{QD} = 1.155/d_{QD}^2$. First, we consider QDs with a surface density matching that of the impurities in graphene. We use PbS nanocrystals capped with PEG500 molecules (QD_{PEG500}) that have effective QD diameter $d_{QD_{PEG500}} \approx 14$ nm, hence surface density $N_{QD_{PEG500}} \approx N_{imp}$ (see experimental section). In these devices, the shift of the minimum of the current-gate voltage curve, $I(V_g)$, demonstrates clearly a reduction of the carrier concentration from $p_0 = 1.7 \times 10^{16}\,m^{-2}$ to $p \approx 0$ and an increase of the field-effect mobility from $\mu_{pristine} = 0.5\,m^2\,(Vs)^{-1}$ to $\mu_{PEG500} = 2\,m^2\,(Vs)^{-1}$ (figure 3(b)). These values of mobility are determined from the $I(V_g)$ curve using the model described in [6]. This 4-fold increase of carrier mobility agrees well with the results of our charge correlation model using the correlation parameter $\beta \approx 0.8$, $r_{max} \approx 10$ nm and $z_{QD} \approx 5$ nm. These parameters correspond to an average in-plane separation between the QDs and the impurity $d_{min} \approx 3$ nm (figure S5, supplementary information S3).

The results for SLG decorated with a layer of smaller QDs, i.e. with higher surface density than N_{imp}, are different. For this experiment we use PbS quantum dots capped with short capping molecules, QD_{TGL}, with $d_{QD_{TGL}} \approx 5$ nm. We observe the carrier concentration

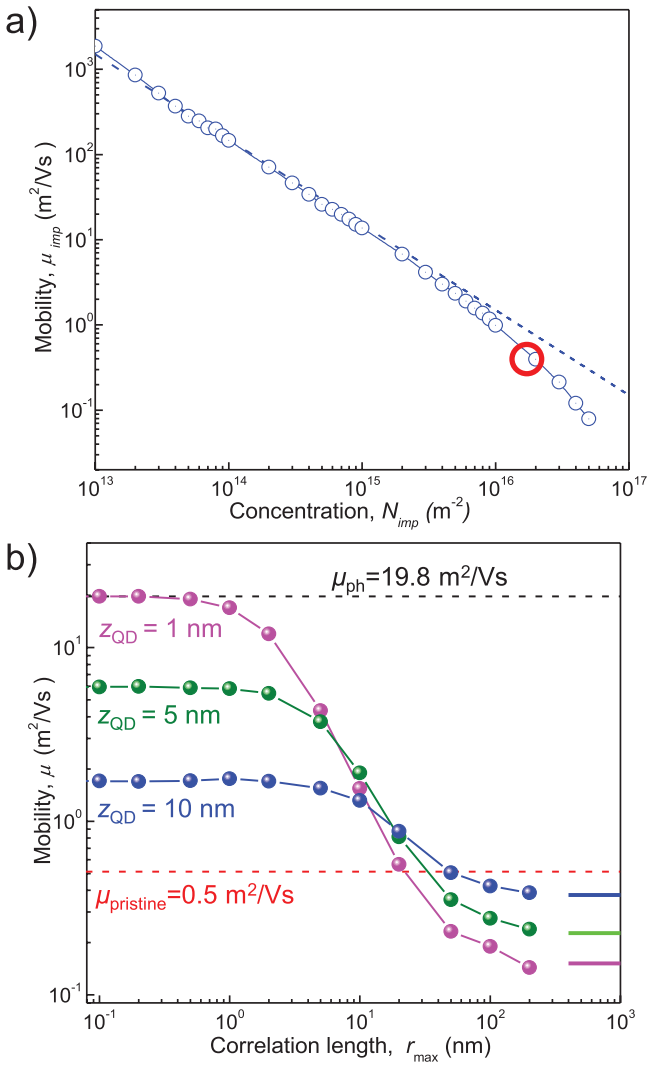

Figure 2. (a) Impurity-limited mobility, μ_{imp}, as a function of impurity density, N_{imp}, calculated by Monte Carlo simulations (data points) and by an analytical model with phenomenological parameter $\alpha = 150$ (dashed line). The red circle corresponds to the mobility of the pristine graphene sample. (b) Calculated mobility, μ, as a function of the correlation length, r_{max}, for a QD concentration $N_{QD} = N_{imp} = 1.7 \times 10^{16}\,m^{-2}$, and stand-off distance $z_{QD} = 1$ nm (magenta), $z_{QD} = 5$ nm (green) and $z_{QD} = 10$ nm (blue). Bold horizontal lines indicate corresponding mobilities in case of no correlation ($r_{max} > 100$ nm). The top dashed line describes the estimated phonon-limited mobility of pristine graphene. The bottom dashed line is the mobility of the pristine graphene sample.

and polarity change from $p = 1.7 \times 10^{16}\ m^{-2}$ to $n = 1.8 \times 10^{16}\ m^{-2}$, accompanied by a mobility increase from $\mu_{pristine} = 0.5\ m^2\ (Vs)^{-1}$ to $\mu_{TGL} \approx 0.7\ m^2\ (Vs)^{-1}$ (figure 3(c)). We attribute the change of conductivity from p to n in this sample to a charge transfer effect: the QDs act as donors with an effective sheet density estimated for hexagonal packing $N_{QD_{TGL}} = 3.5 \times 10^{16}\ m^{-2}$. This is significantly higher than N_{imp}. We estimate that about 50% of ionised QD_{TGL} compensate all the ionised impurities in SLG, while the remaining ionised QDs act as scattering centres. Hence the increase of carrier mobility measured in this device is lower than for devices decorated with QD_{PEG500} for which $N_{QD_{PEG500}} \approx N_{imp}$. For all our devices we find good agreement between the QD areal density and the QD-induced change of carrier concentration in SLG (figure 3(a)), assuming transfer of 1 electron per QD. A small deviation between the QD density and our measured carrier densities for long C-chain ligands could be due to compression and/or interdigitation of capping molecules [25, 26], leading to a higher QD density than that expected for stretched ligands. This observation is also supported by our TEM studies [19], where for PEG-capped QDs the nanocrystal separation distance is smaller. Our TEM studies indicate that the distance can vary from $1l$ to $2l$. Also, although the charge transfer into the adjacent SLG is expected to be faster for shorter ligands [24], we observe kinetic-related effects only in measurements relying on transfer of photoexcited charges [19].

To interpret our experimental results, we plot the calculated dependence of μ on the carrier concentration estimated as $N_{imp} - N_{QD}$, for different correlation lengths, r_{max} (figure 4). Here the results of the Monte Carlo simulations are shown for $r_{max} = 5$ nm (blue), $r_{max} = 10$ nm (green), $r_{max} = 20$ nm (red), and $r_{max} = 30$ nm (magenta). The dashed lines represent the impurity-limited mobility calculated using equation (1)

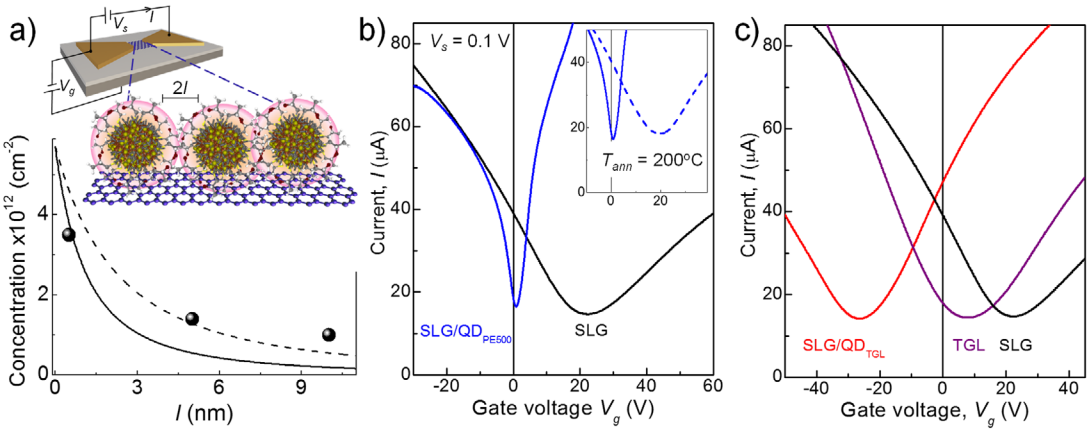

Figure 3. (a) The correlation between the measured QD-induced doping concentration and the areal QD density calculated assuming stretched ligand length, l (black line) and shortened to $l/2$ (dashed line). Inset shows a cartoon of a two-terminal CVD-SLG device decorated with colloidal quantum dots. (b) $I(V_g)$ characteristics of SLG devices before (black line) and after decoration with QD_{PEG500} (blue line). The inset shows the effects of ligand removal by thermal annealing at $T_{ann} = 200$ °C for 1 h on $I(V_g)$ characteristics of the QD_{PEG500} decorated device (dashed line). (c) Effect of surface decoration with a layer of QD_{TGL} (red line) on the $I(V_g)$ characteristics of CVD-SLG devices.

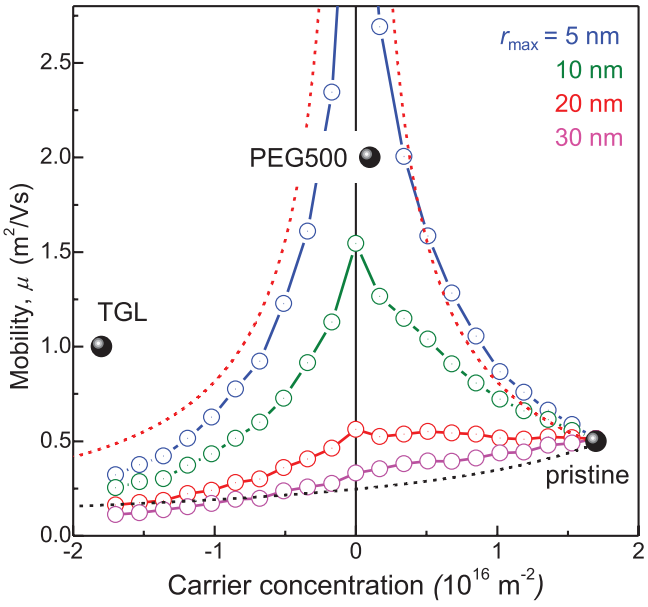

Figure 4. Measured and calculated mobility, μ, as function of carrier density. Black squares are data points for 3 measured devices (pristine, PEG500, and TGL). Circles correspond to Monte Carlo simulations for $z_{QD} = 1$ nm and correlation lengths $r_{max} = 5$ nm (blue), $r_{max} = 10$ nm (green), $r_{max} = 20$ nm (red), and $r_{max} = 30$ nm (magenta). Dashed lines represent results of analytical calculations for maximum and minimum correlation cases with concentration of scattering centres $|N_{imp} - N_{QD}|$ (red line) and $N_{imp} + N_{QD}$ (black line).

with $\alpha = 150$ for two cases: (i) maximum correlation between QD charges and impurities (red line) so that effective concentration of scaterring centers is $|N_{imp} - N_{QD}|$ and (ii) no correlation (black line) with concentration of scatterring centers $N_{imp} + N_{QD}$. We find that the analytical model and the Monte Carlo simulations are in good agreement. Also, they reveal significant asymmetry of the carrier mobility at negative (n-type) and positive (p-type) carrier concentrations in SLG (figure 4). This asymmetry can be explained as follows. Varying the concentration of the donor QDs acts to either increase or decrease the concentration of scattering centres. Also, depending on the degree of correlation between the QDs and impurity charges, the mobility can either increase or decrease relative to the value in pristine graphene.

Our experimental results support the simulations. The largest increase of μ by a factor of 4 is observed for QD_{PEG500} for which $N_{QD_{PEG500}} \approx N_{imp}$. For the SLG decorated with smaller QD_{TGL}, where $N_{imp} < N_{QD}$, the increase of μ is smaller. Also, in this sample the experimental mobility is higher than the calculated value. We envisage that this difference could arise from specific assumptions in our model. We assume an equal contribution to charge scattering from impurities and QD charges. However, there is significant uncertainty

in the value of z_{QD} and it is likely that the charges in the QDs are at larger distance from the SLG than z_{imp}.

Finally, in order to distinguish between the effect induced by capping ligands and by the inorganic nanocrystals on the charge correlation, we use two approaches: first by thermal annealing of QD-decorated devices to remove the capping ligands and secondly by depositing a layer of capping molecules that precedes the deposition of QDs. Thermal annealing of the QD-SLG structures at temperatures up to $T = 200\,^{\circ}C$ for up to 2 h in vacuum leads to the removal of the capping molecules while the crystallinity of the QDs is not affected [27]. This affects the integrity of dielectric layer resulting in significant changes in the electrostatics and hence a reduced spatial correlation of charges and a corresponding decrease of mobility (see inset in figure 3(b) for results on annealing of SLG/QD_{PEG500}). We also note that the deposition of a layer of capping molecules (purple line in figure 3(c)) does not lead to a pronounced increase in mobility, despite the low carrier concentration in the device (the minimum of conductance approaches $V_g \sim 0$ V). This observation suggests that there is no charge correlation effect in organic layer-decorated SLG and that the only deposition of a layer of QDs efficiently capped with ligands leads to significant increase of the carrier mobility by means of charge correlation.

In summary, we have demonstrated that the decoration of single-layer CVD graphene with a layer of ligand-capped QDs has a strong influence on carrier density and provides a means of increasing significantly the carrier mobility even in heavily doped SLG. We have used Monte Carlo simulations combined with a simple electrostatic model to explain this phenomenon by spatial correlation between positive and negative scattering centers in the vicinity of single layer graphene. The control of the carrier concentration and carrier mobility could prove to be a useful tool for fundamental studies of charge correlation phenomena and for the application of graphene in devices requiring a high mobility and controlled carrier concentration.

Experimental section

Single layer graphene on copper substrates was grown by low-pressure chemical vapour deposition (LP-CVD) [18] and transferred onto a SiO_2/n-Si substrate (SiO_2 layer thickness $t = 300$ nm). CVD SLG was processed into 2-terminal planar devices with dimensions of 6 μm $\times$ 10 μm (figure 3). The bottom n-Si layer served as a gate electrode. Colloidal quantum dots with an average PbS core diameter of 4 $\pm$ 1 nm were capped with ligands of different length, l, which determines the effective separation between the PbS nanocrystals and graphene layer [19]. For QD_{PEG500}, the polyethylene glycol (PEG500) has length $l = 5$ nm. For QD_{TGL}, the thioglycerol (TGL) and 2,3-dimercapto1-propanol (DTG) ligands have $l = 0.5$ nm [19]. The QDs were drop-cast from aqueous solution (5 mg ml^{-1}) and dried for 12 h in vacuum. All electrical measurements on two terminal devices were performed at room temperature in vacuum (~10^{-6} mbar).

Acknowledgments

The work is supported by The Leverhulme Trust [grant number RPG-2013-242], the Engineering and Physical Sciences Research Council [grant number EP/M012700/1], the EU Graphene Flagship and The University of Nottingham. Authors acknowledge useful discussions with Dr M Greenaway, Professors M Fromhold, P Beton and N R Thomas. We express our gratitude to Dr A Marsden and N R Wilson for providing CVD graphene; and Dr S Svatek and Dr C Mellor for device processing.

References

[1] Vicarelli L, Vitiello M S, Coquillat D, Lombardo A, Ferrari A C, Knap W, Polini M, Pellegrini V and Tredicucci A 2012 *Nat. Mater.* **11** 865
[2] Konstantatos G, Badioli M, Gaudreau L, Osmond J, Bernechea M, Garcia de Arquer F P, Gatti F and Koppens F H L 2012 *Nat. Nanotechnol.* **7** 363
[3] Zhang D, Gan L, Cao Y, Wang Q, Qi L and Guo X 2012 *Adv. Mater.* **24** 2715
[4] Liu F, Song S Y, Xue D and Zhang H 2012 *Adv. Mater.* **24** 1089
[5] Novoselov K S, Fal'ko V I, Colombo L, Gellert P R, Schwab M G and Kim K 2012 *Nature* **490** 192
[6] Morozov S V, Novoselov K S, Katsnelson M I, Schedin F, Elias D C, Jaszczak J A and Geim A K 2008 *Phys. Rev. Lett.* **100** 016602
[7] Cernetic N, Wu S, Davies J A, Krueger B W, Hutchins D O, Xu X, Ma H and Jen A K-Y 2014 *Adv. Funct. Mater.* **24** 364
[8] Zhang X, Hsu A, Wang H, Song Y, Kong J, Dresselhaus M S and Palacios T 2013 *ACS Nano* **7** 7262
[9] Yager T *et al* 2013 *Nano Lett.* **13** 4217
[10] Song H S, Li S L, Miyazaki H, Sato S, Hayashi K, Yamada A, Yokoyama N and Tsukagoshi K 2012 *Sci. Rep.* **2** 337
[11] Suk J W, Lee W H, Lee J, Chou H, Piner R D, Hao Y, Akinwande D and Ruoff R S 2013 *Nano Lett.* **13** 1462
[12] Feng T, Xie D, Zhao H, Li G, Xu J, Ren T and Zhu H 2014 *Carbon* **77** 424
[13] Bong J H, Sul O, Yoon A, Choi S-Y and Cho B J 2014 *Nanoscale* **6** 8503
[14] Chen F, Xia J and Tao N 2009 *Nano Lett.* **9** 1621
[15] Choi J-H, Wang H, Ju Oh S, Paik T, Sung Jo P, Sung J, Ye X, Zhao T, Diroll B T, Murray C B and Kagan C R 2016 *Science* **352** 205
[16] Raja A *et al* 2016 *Nano Lett.* **16** 2328
[17] Hwang E H, Adam S and Das Sarma S 2007 *Phys. Rev. Lett.* **98** 186806
[18] Wilson N R *et al* 2013 *Nano Res.* **6** 99
[19] Turyanska L 2015 *Adv. Electron. Mater.* **1** 1500062
[20] Maude D K, Portal J C, Dmowski L, Eaves L, Nathan M, Heiblum M, Harris J J and Beall R B 1987 Investigation of the DX center in heavily doped n-type GaAs *Phys. Rev. Lett.* **59** 815
[21] Chadi D J and Chang K J 1988 *Phys. Rev. Lett.* **61** 873
[22] Adam S, Hwang E H, Galitski V M and Das Sarma S 2007 *PNAS* **104** 18392
[23] Talapin D V and Murray C B 2005 *Science* **310** 86
[24] Peng X, Misewich J A, Wong S S and Sfeir M Y 2011 *Nano Lett.* **11** 4562
[25] Paczesny J, Wolska-Pietkiewicz M, Binkiewicz I, Wadowska M, Wróbel Z, Matula K, Nogala W, Lewinski J and Holyst R 2016 *ACS Appl. Mater. Interfaces* **8** 13532
[26] Justo I, Moreels K, Lambert Z and Hens Y 2010 *Nanotechnology* **21** 295606
[27] Turyanska L, Elfurawi U, Li M, Fay M W, Thomas N R, Mann S, Blokland J H, Christianen P C M and Patanè A 2009 *Nanotechnology* **20** 315604